Kai Meng,
***Xin Hou Wang,**
Qing Guan Chen

College of Textile and Clothing Engineering, Soochow University,
No. 178 East GanJiang Road, Suzhou 215021, China

***College of Textiles, Donghua University,**
No. 2999 North RenMin Road, Shanghai 201620, China

Corresponding author: Kai Meng
E-mail: mk2009@suda.edu.cn,

Analysis and Design of a Broad-Width Coat-Hanger Die in the Melt Blowing Process

Abstract
The coat-hanger die plays the role of distributing the molten polymer uniformly across its width so as to ensure the transverse uniformity of the product in the melt blowing process. This paper focused on the design of a broad- width coat-hanger die through combining multiple single dies. A single coat-hanger die was optimised first based on numerical simulation and multi-membered evolution strategy. Subsequently two optimised coat-hanger dies were combined side by side. A satisfactory coefficient of variation value of 0.7828% at the combined die outlet was obtained through adjusting the position of the joint point. The results indicate the feasibility of designing broad- width coat-hanger die through combining multiple single dies.

Key words: *melts blowing process, coat-hanger die, optimal design, simulations.*

Introduction

Melt blowing is a one-step process to produce nonwoven fabrics from polymers. It has become an important and rapidly growing textile industrial technique because of its ability to produce fabrics with an ultra fine fibrous structure, which are used in a variety of commercial areas such as filtration, sorbent material, and insulation. In the melt blowing process, molten polymer is distributed by a coat-hanger die and extruded out of the capillaries. Then the extruded polymer streams are rapidly attenuated by two converging air jets. Some investigators [1 - 5] focused on research of the complex interactions between the air jets and polymer streams. Some other researchers [6 - 9] concentrated on the design of the coat-hanger die, the performance of which is characterised by the flow uniformity at its outlet. A schematic diagram of a coat-hanger die is shown in ***Figure 1.***

Recently the design of the broad-width coat-hanger die has attracted the attention of some researchers due to the market demand for broad-width meltblown nonwovens. Aswe know, the die height and slot part increases with the die width broader, which will lead to an increase in the equipment area and pressure energy consumption. The more unsatisfactory element is that the distortion of the slot will be serious and consequently the die cannot ensure uniform flow distribution. As for the melt blowing process, the common die width is lower than 3.2 m. As early as in 1993, Allen et al. [10] had been aware of this problem and had developed a multiple metering melt blowing system. Later, double coat-hanger dies used in other process were presented in some patents [11, 12]. All this shows that a feasible method of broaden the coat-hanger die is a combination of multiple dies, instead of broadening a single die alone. However, how to combine the dies and the flow nature in the multiple dies have still not been reported.

Due to the above mentioned, in this paper an optimisation method based on numerical simulation and the evolution strategy (ES) were applied for the first time to design a single coat-hanger die. Subsequently 3D finite element analysis was conducted on the combination of two optimised coat-hanger dies. Finally a method of combining multiple dies was proposed for the purpose of achieving a broad-width coat-hanger die.

Optimisation of a single coat-hanger die

Initial die geometry

It is assumed that the polymer flow in the coat-hanger die is an isothermal steady one, and that the molten polymer is an incompressible power law fluid. The tapered manifold of the die can be determined by ***Equation 1***, which is derived by the one-dimensional analytical method.

$$R(x) = \left[\frac{(3k+1)(L-x)}{\pi(4k+2)}\right]^{k/(3k+1)} \left[\frac{H^{2k+1}}{\sin\alpha}\right]^{1/(3k+1)} \quad (1)$$

Where, R is the radius of the manifold, x the distance from the symmetry plane A-A, k the power law index, L the width of the die, H the slot gap, and α the manifold angle. Pittman [13] gave a careful study on the adaptability of isothermal assumption to the polymer flow in a slit die and pointed out that the isothermal assumption was valid under most processing conditions. The non-Newtonian behaviour of the polymer fluid is considered by the power law model because it is one of the most widely used principles in polymer rheology, and the material of interest, such as PP and LDPE follows this model in a wide range of the shear rate.

It can be seen in ***Figure 1*** and ***Equation 1*** that the die geometry is determined by six parameters: R_i, k, L, H, α and B, where R_i and B represent the radius of the die inlet and the die land height, respectively. References [14, 15] show that the die parameters of H and α have obvious influences on the polymer flowing in the die and, therefore, directly affect the variation in the flow rate at the die outlet. For this reason, parameters H and α are chosen as the objective variables and will be optimised. The other parameters can be given as appropriate. In the case of this work, let L be 200 mm, B - 10 mm, R_i - 4 mm and the polymer material used Exxon MFR35 PP, the value k of which under molten conditions is 0.79.

Optimisation procedures

The objective variables of H and α are optimised by the method of ES refer-

ring to the idea of biological mutation, the history and development of which can be seen in literature [16]. In addition, it is necessary to explain that the ES used in this paper is the so-called multi-membered ES. In our previous paper, a preliminary study was conducted using single-membered ES [9]. The difference between the two types of ES is clearly evident in the operation process, convergence rate, and optimisation results.

Initialisation

The multi-membered ES can be expressed as (μ,λ)-ES, which means that there are μ parents and λ offspring in a generation. Assuming the task is a minimisation problem, the optimisation model can be described as ***Equation 2*** according to our previous paper [9]. Where, $F(H,\alpha)$ represents the objective function. The subject conditions are determined according to the basic die shape. Generally speaking, slot gap H is less than the radius of the die inlet, and the manifold angle α is less than 90°.

$$\begin{cases} \text{Min } F(H.\ \alpha) \\ \text{Subject to } 0 < H < 4,\ 0 < \alpha < 90° \end{cases} \quad (2)$$

The objective variables are described by $X = x_1, x_2, x_i, \cdots, x_n$, where x_i are real variables ($i = 1, 2, \cdots, n$). Each individual corresponds to a vector in n-dimensional space and is characterised by some standard deviation σ_j ($j = 1, 2, \cdots, n$) of normal distribution, which is called the mutation operator and is characteristic of adaptive properties. In this article, the variables are H and α, hence the value of n is 2. Then each individual can be expressed as ***Equation 3***.

$$(X, \sigma) = ((x_1, x_2), (\sigma_1, \sigma_2)) = \\ = ((x_H, x_\alpha), (\sigma_H, \sigma_\alpha)) \quad (3)$$

The initial population contains μ individuals. In the choice of μ and λ there is no rule to follow, and there is no need to ensure that λ is exactly divisible by μ. It is only necessary that λ exceeds μ and $\mu > 1$ in the (μ, λ)-ES. However, the value of μ and λ are relevant to the computing time and convergence rate. The value of f μ and λ are larger, the longer the computing time. Research [17] shows that $\lambda \geq 6\mu$ can speed up the rate of convergence. Therefore, considering the computing time and convergence rate, μ and λ are chosen to be 3 and 18, respectively, in this article. For the purpose of global searching, the initial value of objective variables in μ individuals can be distributed evenly in the searching space. And the initial value of σ_j can be determined according to the specific problem; usually the initial value of σ_j can be equal to 3 [18]. They will be self-adapting in the evolution process, thus the three initial individuals can be formulated as follows:

$$X^1 = ((x^1_H, \sigma^1_H), (x^1_\alpha, \sigma^1_\alpha)) = \\ = ((1, 3), (15°, 3)) \quad (4)$$

$$X^2 = ((x^2_H, \sigma^2_H), (x^2_\alpha, \sigma^2_\alpha)) = \\ = ((2, 3), (45°, 3)) \quad (5)$$

$$X^3 = ((x^3_H, \sigma^3_H), (x^3_\alpha, \sigma^3_\alpha)) = \\ = ((3, 3), (75°, 3)) \quad (6)$$

Recombination

Two parents are selected from the population randomly to recombine into one offspring in the recombination. There are two standard classes of recombination in ES: 'discrete recombination' and 'intermediate recombination'. Beyer and Schwefel [19] recommended that the former is suitable for the objective variables and the latter for the mutation operators. Assuming Parent^1 and Parent^2 are selected randomly from the population, the Offspring is generated as follows:

$$\text{Parent}^1 = (X^1, \sigma^1) = \\ = ((x^1_H, x^1_\alpha), (\sigma^1_H, \sigma^1_\alpha)) \quad (7)$$

$$\text{Parent}^2 = (X^2, \sigma^2) = \\ = ((x^2_H, x^2_\alpha), (\sigma^2_H, \sigma^2_\alpha)) \quad (8)$$

$$\text{Offspring} = (X, \sigma) = \\ = (x^{qi}_H, x^{qi}_\alpha), \left(\frac{\sigma^1_H + \sigma^2_H}{2}, \frac{\sigma^1_\alpha + \sigma^2_\alpha}{2}\right) \quad (9)$$

Where, qi is equal to 1 or 2 randomly.

Mutation

The offspring generated by the recombination will be mutated as follows:

$$\sigma'_H = \\ = \sigma_H \cdot \exp(\tau_0 \cdot N(0, 1) + \tau \cdot N_H(0, 1)) \quad (10)$$

$$x'_H = x_H + \sigma'_H \cdot N'_H(0, 1) \quad (11)$$

$$\sigma'_\alpha = \\ = \sigma_\alpha \cdot \exp(\tau_0 \cdot N(0, 1) + \tau \cdot N_\alpha(0, 1)) \quad (12)$$

$$x'_\alpha = x_\alpha + \sigma'_\alpha \cdot N'_\alpha(0, 1) \quad (13)$$

Where, σ'_H and σ'_α represent the standard deviation after mutation, x'_H and x'_α - the new objective variable after mutation, $N(0, 1)$, $N_i(0, 1)$, $N_i'(0, 1)$ - three different normal distributed random numbers, with the value expected being zero and the variance being 1, τ_0 and τ - the learning parameters. The two learning parameters are as follows:

$$\tau_0 = c\Big/\sqrt{2n} \quad \tau = c\Big/\sqrt{2\sqrt{n}} \quad (14)$$

Due to $n = 2$ in this article and the two learning parameters being within the interval 0.1 - 0.2, as usually used in practice, constant $c = 0.3$ is suitable.

Selection

In each generation, repeat the step of recombination and mutation to produce λ offsprings. μ individuals corresponding to a smaller value of the objective function are selected out of λ individuals as the next generation's parents. The value of the objective function can be expressed by the coefficient of variation (CV) value of the flow velocity at the die outlet, which cannot be expressed and calculated by the traditional analytical method accurately. Therefore 3D finite element numerical simulation was used to obtain the velocity field in the coat-hanger die. Details of the simulation process was introduced in our previous paper [9] and will not be repeated here.

Termination condition

From the point of view of the convergence rate and computing time, the terminal condition in this paper is that checking the fitness every 10 generations

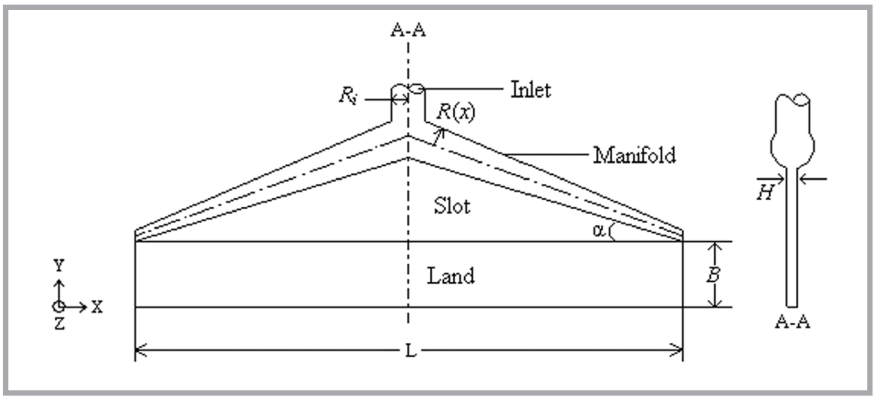

Figure 1. *Schematic diagram of a coat-hanger die.*

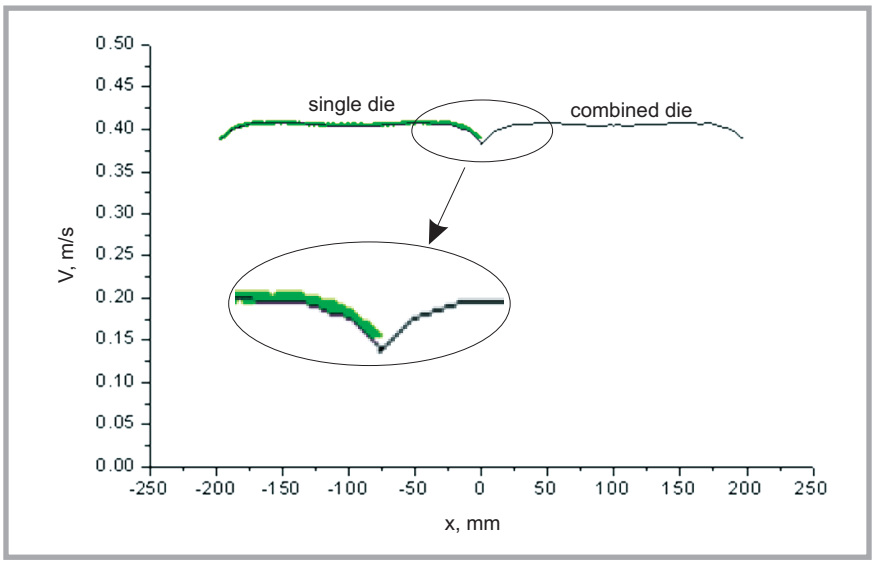

Figure 2. *Velocity distribution at the die outlet.*

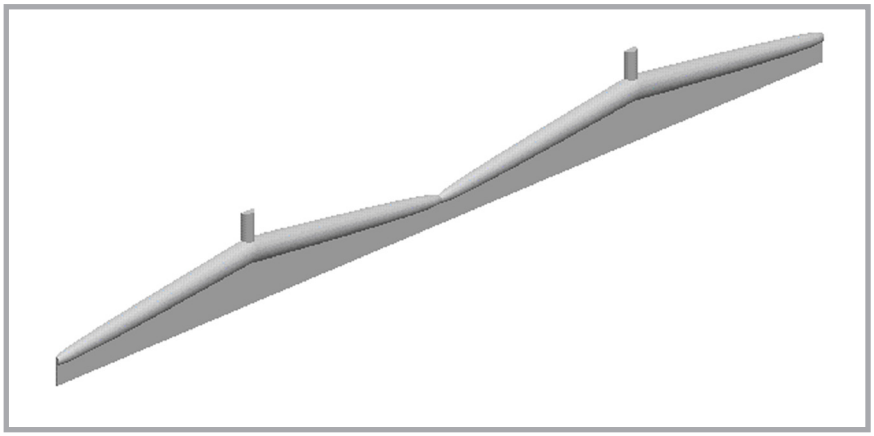

Figure 3. *Geometric model of the combined die.*

in terminates if the optimal fitness in this check is not better than the last one. This actually means that the objective function has no improvement at least in 10 generations.

Optimisation results and discussion

The evolution processes of (3, 18)-ES were stopped at the 30th generation based on the termination condition. The optimal results achieved in every generation are listed in ***Table 1***, including the optimal value of the variables and the CV% value. From ***Table 1*** we can see that (3, 18)-ES achieved the minimum CV% value of 0.9465% at the 19th generation in the whole evolution process, where the objective variables are H = 1.2325 mm, α = 6.4812°, respectively. Comparing the results in reference [9], a lower CV% value was obtained and a short computing time expended in this paper, though the operation process of multi-membered ES is more complex than that of single-membered ES.

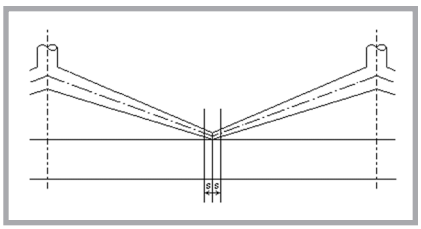

Figure 4. *Combination of two coat-hanger dies.*

Velocity distribution at the die outlet is shown in ***Figure 2*** (indicated by single die), in which x and v represent the distance from the symmetry plane and velocity magnitude, respectively. Since the die opening at the exit is constant across the die width in this case, the velocity distribution also represents the volumetric flow rate distribution. It can be seen that the flow velocity is quite uniform, except the relative lower velocities near the die end. This may result from the no slip boundary conditions on the wall and it is inevitable in the practice. In order to obviate the effect of this distribution, the selvedge of the melt blown nonwovens will be cut away in some cases.

Combination of coat-hanger dies

Two optimised coat-hanger dies are combined into one die side by side. As shown in ***Figure 3***, the combined die has two inlets and one outlet, the height of which is the same as a single die, but the die width is doubled. Polymer flow in the combined die was also simulated by using the 3D finite element method. Velocity distribution at the combined die outlet is also shown in ***Figure 2*** (indicated by the combined die) for the convenience of comparison. Comparing the two curves in ***Figure 2***, it seems that the combined die is just a combination of two coat-hanger dies. However, it is found that velocities near the joint point are lower than those of the same position at the single die, leading to an increase in the CV% value at the combined die outlet to 1.1241%. On the other hand, lower velocities near the joint point are exactly in the middle of the combined die outlet, which cannot be obviated by cutting away the selvedge

Table 1. *Optimal results in every generation.*

Generation	H, mm	α, °	CV, %
1	2.6014	41.0716	4.0138
2	2.3290	46.0875	5.1292
3	2.6738	44.1969	6.3107
4	2.6418	38.7971	4.6972
5	2.4823	35.7771	3.1991
6	2.1736	28.4442	9.2299
7	2.4317	28.0779	2.6333
8	2.4458	26.7210	3.1659
9	2.2128	24.9670	5.1643
10	2.3143	27.2889	3.9411
11	2.2324	20.4108	2.5581
12	2.0036	17.5236	2.8258
13	2.4553	27.6358	2.9590
14	1.8298	13.3214	1.4412
15	0.6770	2.9807	1.7835
16	1.1499	5.5271	1.8941
17	1.5320	10.0985	2.0148
18	1.5684	9.8004	1.1814
19	1.2325	6.4812	0.9465
20	1.7740	14.9036	5.3447
21	1.2474	7.5238	3.0934
22	0.8786	3.6667	2.2546
23	1.6102	10.3928	0.9824
24	1.6177	11.0565	1.2211
25	0.9216	3.7987	2.5985
26	1.3280	7.3098	1.0997
27	1.2872	6.6679	1.5846
28	1.2576	6.6309	1.0689
29	1.2742	6.3182	2.3079
30	1.4298	9.1017	2.4277

Table 2. Four schemes of combination.

Single die width, mm	s, mm	Percentage, %	Combined die width, mm	CV, %
200	0	0.0	400	1.1241
	1	0.5	398	0.7828
	2	1.0	396	0.8574
	3	1.5	394	1.0484

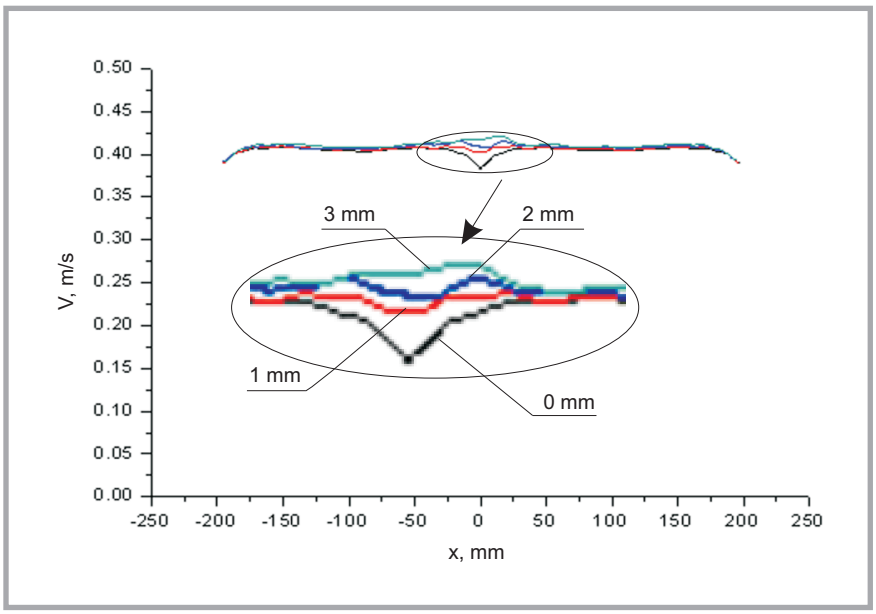

Figure 5. *Velocity distribution at different combined die outlets.*

and will be certain to affect the uniformity of the product. Therefore, lower velocities near the joint point need to be eliminated.

From ***Figure 2*** we can see that the lower velocities near the joint point originate in the lower velocities near the single die end. Therefore, the 'wing shape' velocity distribution may be eliminated if the die end was modified. Just as ***Figure 4*** illustrates, we try to discard a fraction of each single die end *s* when combining the two coat-hanger dies. ***Table 2*** lists the four schemes as well as the corresponding CV% value. ***Figure 5*** shows the velocity distribution corresponding to the four schemes. From ***Table 2*** and ***Figure 5*** it can be seen that the CV% value first decreases and then increases with an increase in *s*, meanwhile the velocity distribution changes from a concave shape to a convex one. We can predict that the velocity distribution will be more uniform if the value of *s* is between 1 mm and 2 mm. However, it is unnecessary to spend much time seeking an optimal *s* between 1 mm and 2 mm, the reason for which being that scheme 2 is good enough from the point of view of the CV% value and velocity distribution. On the other hand, there may not be an obvious decrease in the CV% value because of the small interval of scheme 2 and scheme 3. In addition, we should emphasis that the plots in ***Figure 5*** are not symmetrical with respect to the x = 0 joint point, especially in the case of a large value of *s*. This is because the flow velocity and angle of collision of the two streams at the joint point increase with an increase in *s*, which can easily lead to an asymmetrical flow.

Three coat-hanger dies were also combined and analysed. Results show that the flow nature near the joint point is similar to the description above. Therefore, a workable broad-width coat-hanger die can be designed through combining multiple dies under conditions of adjusting the joint point properly. However, it should be noted that the width of the combined die and number of single dies should be determined according to the process capability in practice.

Conclusions

A single coat-hanger die was optimised to distribute molten polymer uniformly across the die outlet. The CV% value at the optimised coat-hanger die outlet can reach 0.9465% in this case. A workable broad-width coat-hanger die can be designed through combining multiple optimised dies under conditions of adjusting the joint point properly. The combination of two optimised coat-hanger dies shows that the CV% value can decrease to 0.7828% when the joint point is in the position of 1 mm from the die end in this case.

Acknowledgments

This work was supported by the National Natural Science Foundation of China (Grant No. 51106102).

References

1. Lewandowski, Z.; Ziabicki, A.; Jarecki, L. *Fibres and Textiles in Eastern Europe*, 2007, 15, 5-6 (64-65), 77.
2. Jarecki, L.; Ziabicki, A. *Fibres and Textiles in Eastern Europe*, 2008, 16, 4 (70), 17.
3. Jarecki, L.; Lewandowski, Z. *Fibres and Textiles in Eastern Europe*, 2009, 17, 1 (72), 75.
4. Krutka, H. M.; Shambaugh, R. L.; Papavassiliou, D. V. *Ind. Eng. Chem. Res.*, 2008, 47, 935.
5. Sinha-Ray, S.; Yarin, A.L.; Pourdeyhimi, B. *J. Appl. Phys.*, 2010, 108, 034912-1.
6. Huang, Y. H.; Gentle, C. R.; Hull, J. B. *Adv. Polym. Tech.*, 2004, 23(2), 111.
7. Meng, K.; Wang, X. H.; Huang, X. B. *J. Appl. Polym. Sci.*, 2008, 108(4), 2523.
8. Lebaal, N.; Schmidt, F.; Puissant, S. *Finite Elem. Anal. Des.*, 2009, 45, 333.
9. Meng, K.; Wang, X. H., Huang, X. B. *Polym. Eng. Sci.*, 2009, 49 (2), 354.
10. US Patent 5,236,641 (1993).
11. US Patent 6,491,507 B1 (2002).
12. CN Patent 200720305512.4 (2008).
13. Pittman, J. F. T.; Sander, R. *Int. Polym. Process,* 1994, 4, 326.
14. Non, S. Y.; Kim, D. H. Korean, J. *Chem. Eng.*, 1995, 12(2), 236.
15. Chen, C.; Jen, P.; Lai, F.S. *Polym. Eng. Sci.*, 1997, 37(1),188.
16. Schwefel, H.-P. Evolution and Optimum Seeking, *Wiley-Interscience*, 1995, 105-162.
17. Schwefel, H.-P. Numerical Optimization of Computer Models, John Wiley & Sons, Chichester, 1981, 153.
18. Rodzin, S. I. IEEE International Conference on Artificial Intelligence Systems, Divnomorskoe, Russia, Schemes of Evolution Strategies, 2002, 375.
19. Beyer, H.-G.; Schwefel, H.-P. Natural Computing, Kluwer Academic Publishers, Netherlands, 2002, 18-22.

Received 13.01.2011 Reviewed 08.09.2011